Long-term Hydrographic Variability in the Northwest Pacific Ocean

Terrence M. Joyce and Jane Dunworth-Baker

Woods Hole Oceanographic Institution
Woods Hole, Massachusetts

Abstract. Hydrographic changes in the Northwest Pacific Ocean are examined using data for two time periods: 1945: 1975 and 1976:1998. The largest changes in T/S (2°C,0.2 psu) are within the inter-frontal zone between the Kuroshio Extension (KE) and the subarctic (or Oyashio) front near the Shatsky Rise, and are consistent with a southward shift of the Kuroshio Bifurcation Front (KBF). Other major changes seen are a freshening of approximately 0.04 psu of the newly formed North Pacific Intermediate Water (NPIW); a shoaling over time of the halocline in the center of the Western Subarctic Gyre (WSAG); and a southward shift of the subarctic front between the dateline and 150°W. Because long-term T/S changes near the Shatsky Rise are well correlated, we have examined subsurface thermal data at 100 and 200-m depth in the region and found that shifts in front locations show a high degree of correlation with the Pacific Decadal Oscillation index on an inter-annual basis, and lag that index by about one year at 200-m depth.

1. Introduction

Studies of interannual to decadal timescale variability in the NW Pacific have generally utilized sea surface temperature or subsurface temperature. Our interest is to take advantage of a new summary of the hydrography in the N. Pacific (Macdonald *et al.*, 2001), updated here with recent data from the World Ocean Circulation Experiment (WOCE), which allows hydrographic data to be combined and analyzed by grouping and averaging on potential density surfaces. Macdonald *et al.* presented a hydrographic climatology and our intent is to explore variability. However, the availability of hydrographic data for a study of temporal variability is much less than for subsurface temperature data (from MBTs and XBTs), and we have therefore chosen to examine only two time periods and the changes between them. The time periods are 1945:1975 and 1976:1998, spanning what has been come to be called a major regime shift (Trenberth, 1990; Mantua *et al.*, 1997) in the atmosphere, ocean and biology of the North Pacific. While we concentrate on temperature and salinity changes, other hydrographic data are available and have been used to examine changes over time, such as dissolved oxygen and silica.

2. Hydrographic Changes

Hydrographic station data for each of the two periods (Figure 1) show a high density of observations near Japan decreasing to the east. In the latter period (containing WOCE data), the data coverage is clearly biased along 'lines' with little or no data in between. Clearly, the estimation of spatial changes must address this sampling problem and one may consider two choices: comparison of changes along synthetic hydrographic 'sections' or spatially interpolating onto a rather coarse grid. We chose the latter and used a nearest neighbor method with a 5° resolution in latitude and longitude, then interpolating onto a finer grid for comparison and display. Thus, we will be examining rather broad scale changes between the two time periods. We have chosen to show T/S fields and differences at two depths: 100 and 200 m (Figure 1). Dynamic height fields and differences are shown for the surface relative to a 1000-dbar pressure surface.

We begin with dynamic height, which shows the mean (1945:1998) baroclinic surface height structure of the KE and the WSAG with a minimum height SE of Kamchatka and a maximum height south of Japan. The temporal change in dynamic height is plotted along with mean frontal locations of the KE (using the 12°C isotherm at 300 m following Mizuno and White, 1983) and the subarctic front or Oyashio boundary (using the 33.6 psu salinity at 100 m following Kawai (1972) and there is clear evidence that major changes in dynamic height follow the fronts. A southward shift of the axis of the KE is indicated by negative dynamic height anomalies of 5–10 cm along its axis. These dynamic height changes are largest to the west of the dateline and are supported by T/S changes. One can see evidence for a southward shift of the Oyashio front between the two periods in the region to the east of the dateline to at least 150°W, the eastern boundary of our domain; this is seen by a negative salinity (and temperature) change along the northern of the two fronts plotted in Figure 1.

The largest T/S changes occur in the zone between the two fronts centered roughly at 160°E. Kawai cites a paper dating back to Uda in 1935 where it was first shown that various fronts split apart, with a major bifurcation of the Kuroshio Extension (Kuroshio Bifurcation Front: KBF) occurring near the Shatsky Rise at 155°E. A northern branch of this front then merges with the Oyashio to become a subarctic front to the east. This region of bifurcation in the KE was examined in detail by Mizuno and White (1983) in their analysis of five years of XBT data between 1976 and 1980. They interpret their data as reflecting temporal shifts in the thermal structure of the KE and link location of bifurcations of the KE with the topography of the Shatsky Rise following Levine and White (1983). Another study by Belkin and Mikhailichenko (1986) specifically targeted this longitude in a high-resolution hydrographic survey interpreted in terms of synoptic frontal locations. We find that long-term salinity changes are consistent with the interpretation of dominant changes in time at both 100-m and 200-m depth being due to meridional shifts of fronts. Since T/S changes are well correlated this will allow us in the next section to interpret temperature changes alone in terms of meridional shifting of fronts rather than diabatic forcing near 160°E.

In Figure 1, the local maximum in mean salinity at 200 m, SE of Kamchatka, is within the WSAG and reflects a shallower halocline near the gyre center; it is co-located with the minimum in mean dynamic height. In the same region, there is a salinity increase with time at both depths due to the shoaling of the halocline, a reduction of 5 cm in surface dynamic height over time with perhaps some suggestion of a westward intensification, but no noticeable temperature change. The salinity increase at 100 m extends into the eastern subpolar gyre as well. In summertime, a distinct temperature minimum layer develops in this region (see Talley et al, 1990 for a hydrographic section in the region) centered near a depth of 100 m, making temperature a poor 'tracer' for vertical motion. Strong vertical gradients in dissolved oxygen and silica exist in this region in the upper ocean and, indeed, silica increases over time while oxygen decreases (neither is shown here) consistent with this interpretation of salinity change. Changes in halocline depth over time are consistent with a spinning up of the subpolar gyre(s), and will be discussed later.

We also have investigated the changes in NPIW between the two periods (Figure 2) and have found it to be freshening by approximately 0.04 psu. This analysis was done on a potential density surface of 26.8, which is the climatological level at which this water mass is formed by subsurface mixing processes (Talley, 1993) between source waters in the Sea of Okhotsk and the Kuroshio. The core thickness of this layer can be traced by its planetary potential vorticity (Yasuda, 1997) from the Sea of Okhotsk (Figure 2, upper panel) as it moves into the interfrontal zone where it first appears as a sub-surface salinity minimum. Between the two time periods, this layer has freshened (Figure 2, lower panel) over much of its pathway, with the greatest freshening within the inter-frontal zone, not in the Sea of Okhotsk. If this freshening were due to an increase in transport of the subarctic gyre, bringing more subpolar water into the KE, one would expect the dissolved oxygen of the layer to increase in time, but in fact it decreases (not shown). Thus, NPIW changes are not simply linked to wind-driven transport changes, and could also depend upon long-term changes in the net freshwater flux in the subpolar North Pacific, as suggested by Wong *et al.*, (1999) with lower-salinity water in the surface layer reducing ventilation by vertical diffusion, as reflected in changes in the oxygen concentration at depths near a potential density of 26.8. Indeed, the oxygen in the Sea of Okhotsk is lower at this density in the second period.

3. Subsurface Temperature Changes

Because the long-term changes in subsurface temperature at depths of 100 and 200 m are so well correlated with salinity, it is sensible to ask if the more numerous temperature data may now be interpreted in terms of what we have seen from the hydrography. All available MBT and XBT data have been extracted from the WOD98-05 (Conkright *et al.*, 1998). These have been augmented by more recent data from the Global Temperature and Salinity Pilot Project (GTSPP: available at http://www.nodc.noaa.gov/GTSPP/gtspp-bc.html) up through and including 1999. They have been gridded annually and with a resolution of 1° of latitude and 2° of longitude. Interannual anomalies have been calculated and for our purposes here, averaged for a box region between 154: 166°E and 36:42°N, suggested by the 'bullseye' temperature difference in Figure 1. In fact, this region was one with a local maximum in interannual variability for temperature at 100 and 200-m depths for the time period 1954:1999. We have seen (not shown) that compositing the data before and after 1976 produced a similar, temperature difference as found with the hydrography. The advantage of the thermal data is greater temporal resolution than with the hydrography. We have done this (Figure 3) for both depths analyzed above and plotted a filtered PDO index following Mantua *et al.*, smoothed in time with a running 3-point .25, .50, .25 filter. One can see clearly that subsurface thermal anomalies are highly correlated with one another and anti-correlated with the PDO (r = -0.8), lagging the latter by about a year (not shown), with a suggestion of a longer lag with increasing depth. Since 100 m lies within the winter mixed layer, temperature changes at this depth may be due to surface forcing as well as meridional shifts of water masses. A depth of 200 m lies below mean winter mixed layer depths in the region (Huang and Qiu, 1994) and is less susceptible to diabatic effects. The 'regime shift' is one of predominantly low-to-high PDO index, but with interannual variations that are reflected in both the index and the subsurface temperature field. The period over which Mizuno and White did their analysis (1976–1980) is one of small change relative to the whole record. The meridional amplitude or zonal extent of the branching of the KBF as reflected in Figure 3 is highly time-dependent and linked to ocean dynamics associated with the PDO.

4. Discussion

Recently Deser *et al.* (1999) examined 50-m and 400-m temperature variability for the period of 1968:1991 spanning the regime shift in the PDO or the North Pacific Index (NPI), after Trenberth and Hurrell (1994). The NPI is based on SLP variations off the Aleutians, and is not a SST-based index like the PDO, but the two indices are highly anti-correlated. Deser et al found that leading EOFs were correlated with the intensity of the Aleutian low, with 50 m nearly in phase and the 400-m temperature lagging by about 4 years, bracketing the one year lag at 200 m of our simple temperature box centered at 39°N, 160°E. The spatial EOF pattern at the two depths was substantially different, however, with the 50-m EOF centered on the dateline and the 400-m off the east coast of Japan: again bracketing our Shatsky Rise location. Deser *et al.* further examined wind stress variability and showed that there were changes in the Sverdrup circulation associated with the NPI changes, with low PDO (high NPI) periods ones with reduced wind-driven transport and the opposite during periods of high PDO (low NPI). Miller et al (1998) composited data from 1970:1976 and 1980:1986 and explored changes in thermocline depth (400 m) using data and a coarse-grid wind-driven model. They found that the model produced westward-intensified variability between these periods in agreement with the data and the second period was one of increased transports in both the subarctic and subtropical gyres. This spin-up of the subarctic region is consistent with the above changes in salinity, dynamic height, oxygen and silica in the center of the WSAG.

Diabatic effects were the focus of a study by Yasuda and Hanawa (1997), who had a particular interest on mode waters of the North Pacific, and they found that the strong SST signal near the dateline was produced by a combination of changes in air–sea heat flux and Ekman layer transport of heat, with enhanced production of central mode water during the years following the regime shift. While they did not comment, their data showed the maximum temperature change at depths of 100– 300 m was located over the Shatsky Rise in the region of the KBF (their Figure 2 at 39°N), not in the region of mode water formation

The analysis of section data at 137°E by Qiu and Joyce (1992) indicated an increase in Kuroshio geostrophic transport of about 10 Sv for the period after the regime shift compared to the period before; but this time series is too short to make any definitive statement about time lags relative to the PDO. Kuroshio transport must be closely related to dynamic height changes associated with thermocline adjustments, and therefore the 400-m temperature changes analyzed by Deser et al and Miller *et al.* Yet changes at this depth lag those at 200 m. If the latter are independent of diabatic effects and thus associated with frontal positions as we have argued, they precede changes at 400 m in time. It appears that wind-driven transport of the North Pacific is probably the single most important driver of the long-term hydrographic changes observed in this study, and that meridional shifts in fronts are important in creating changes in the location of water masses, hence hydrographic variability in the Northwest Pacific. The phasing of the changes suggest, however, that shifts in the KBF and perhaps other fronts may not result from a change in an upstream transport condition near Japan but from adjustment to wind-driven changes coming from the east.

The evolution of NPIW towards colder, fresher characteristics does not seem simply related to wind-driven transport changes between the two periods. An increase in the subpolar component of NPIW would increase the contribution of fresher end-member which mixes with the warmer, saltier Kuroshio waters in the KE (e.g., See Joyce *et al.*, 2001). However, oxygen content changes are not consistent with this. Neither is a simple change in properties of the low PV source water in the Sea of Okhotsk, as salinity changes there are small.

Acknowledgments. This work was part of a JAMSTEC project at WHOI aimed at identifying sites for long-term monitoring in the NW Pacific, under the leadership of Sus Honjo. We also acknowledge an exchange of ideas with K. Hanawa, T. Suga, B. Qiu, and R. Krishfield and two anonymous reviewers during the course of this work.

References

Belkin, I.M., and Yu.G. Mikhailichenko, 1986. Thermohaline structure of the Northwest Pacific Frontal Zone near 160°E. *Oceanology*, English translation, **26**, 47–49.

Conkright, M.E, S. Levitus, T.P. Boyer, T. O'Brien, C. Stephens, D. Johnson, L. Stathoplos, O. Baranova, J. Antonov, R. Gelfeld, J. Burney, J. Rochester, C. Forgy, 1998. Temperature, Vol 5, World Ocean Database 1998 CD-Rom Scientific Dataset, version 1.0. National Oceanographic Data Center Internal Report 14.

Deser, C.M., A. Alexander, and M.S. Timlin, 1999. Evidence for a wind-driven intensification of the Kuroshio Extension from the 1970s to the 1980s. *J. Climate*, **12**, 1697−1706.

Huang, R.X., and B. Qiu, 1994. Three-dimensional structure of the wind-driven circulation in the subtropical North Pacific. *J. Phys Oceanogr*., **24**, 1608−1622.

Joyce, T.M., I. Yasuda, Y. Hiroe, K. Komatsu, and F. Bahr, 2001. Mixing in the meadering Kuroshio Extension and the formation of North Pacific Intermediate Water, *J. Geophys. Res.*, **106**, 4397–4404.

Kawai, Hideo, 1972. Hydrography of the Kuroshio Extension, In *Kuroshio*, H. Stommel, K. Yoshida, Eds., U. Tokyo Press, 517 pp.

Levine, E.R., and W.B. White, 1983. Bathymetric influences upon the character of North Pacific fronts, *J. Geophys. Res.,* **88**, 9617–9625.

Macdonald, A.M., T. Suga, and R,G. Curry, 2001. An isopycnally averaged North Pacific Climatology. *J. Atmos. and Oceanic Tech*., **18**, 394–420.

Mantua, N.J., S.R. Hare, Y. Zhang, J.M. Wallace, and R.C. Francis, 1997. A Pacific interdecadal climate oscillation with impacts on salmon production. *Bull. Amer. Meteor. Soc*., **78**, 1069–1079.

Miller, A.J., D.R. Cayan, and W.B. White, 1998. A westward-intensified decadal change in the North Pacific thermocline and gyre-scale circulation. *J. Climate*, **11**, 3112–3127.

Mizuno, K., and W.B. White, 1983. Annual and interannual variability in the Kuroshio current system. *J. Phys. Oceanogr*., **13**, 1847−1867.

Talley, L.D., T.M. Joyce, and R.A. DeSzoeke, 1991. Transpacific sections at 47°N and 152°W: distribution of properties. *Deep-Sea Res*., **38**, Suppl., S63−S82.

Talley, L.D., 1993. Distribution and formation of North Pacific Intermediate Water. *J. Phys. Oceanogr*., **23**, 518–537.

Trenberth, K.E., 1990. Recent observed interdecadal climate changes in the Northern hemisphere. *Bull. Amer. Meteor. Soc*., **71**, 988–930.

Trenberth, K.E., and J.W. Hurrell, 1994. Decadal atmosphere–ocean variations in the Pacific. *Climate Dyn.*, **9**, 303−319.

Qiu, B., and T.M. Joyce, 1992. Interannual variability in the mid- and low-latitude western North Pacific. *J. Phys. Oceanogr*., **222**, 1062−1079.

Wong, A.P.S., N.L. Bindoff, and J.A.Church, 1999. Large-scale freshening of intermediate waters in the Pacific and Indian Oceans, *Nature*, **400**, 440–443.

Yasuda, T., and K. Hanawa, 1997. Decadal changes in the Mode Waters in the midlatitude North Pacific, *J. Phys. Oceanogr*., **27**, 858−870.

Yasuda, I., 1997. The origin of the North Pacific Intermediate Water. *J. Geophys. Res.*, **102**, 893−909.

Figure 1. Hydrographic data showing the climatology of dynamic height (0−1000 dbar), temperature and salinity (100 amd 200-m depth) and their long-term changes with time. The white chain-dashed line is the axis of the KE and the dashed line the subarctic or Oyashio front, as discussed in the text. Color bars at the bottom of the panels refer to changes in dynamic height (m, contour interval: 0.05), temperature (°C, contour interval: 1) and salinity (psu, contour interval: 0.1).

Figure 2. The NPIW layer analysis is done on a potential density surface (σ_θ=26.8 kg/m^3), showing mean Potential Vorticity ($\times 10^{-12}$ (ms)$^{-1}$, upper panel, < 150 shaded) and salinity change (psu, lower panel, negative values shaded, 0.02 contours dashed, 0.04 contours solid) between the two periods. The lateral PV minimum waters within the interfrontal zone, reflecting the 'newly formed' NPIW, are everywhere fresher, with relatively large salinity decreases of 0.04 psu. This density layer is at depths of less than 300 m along the Kuril Islands and deepens about 200 m near the dateline along 40°N as it subducts within the interfrontal zone north of the KE, and then another 200 m as it crosses the KE.

Figure 3. Time series of 100-m and 200-m temperature in a 6° (lat) × 12° (lon) box centered at 39°N, 160°E from subsurface temperature data archives. Interannual anomalies are calculated for the region and then spatially-averaged. Also shown is the smoothed Pacific Decadal Oscillation index (based on December−March wintertime SST data) beginning in 1954.

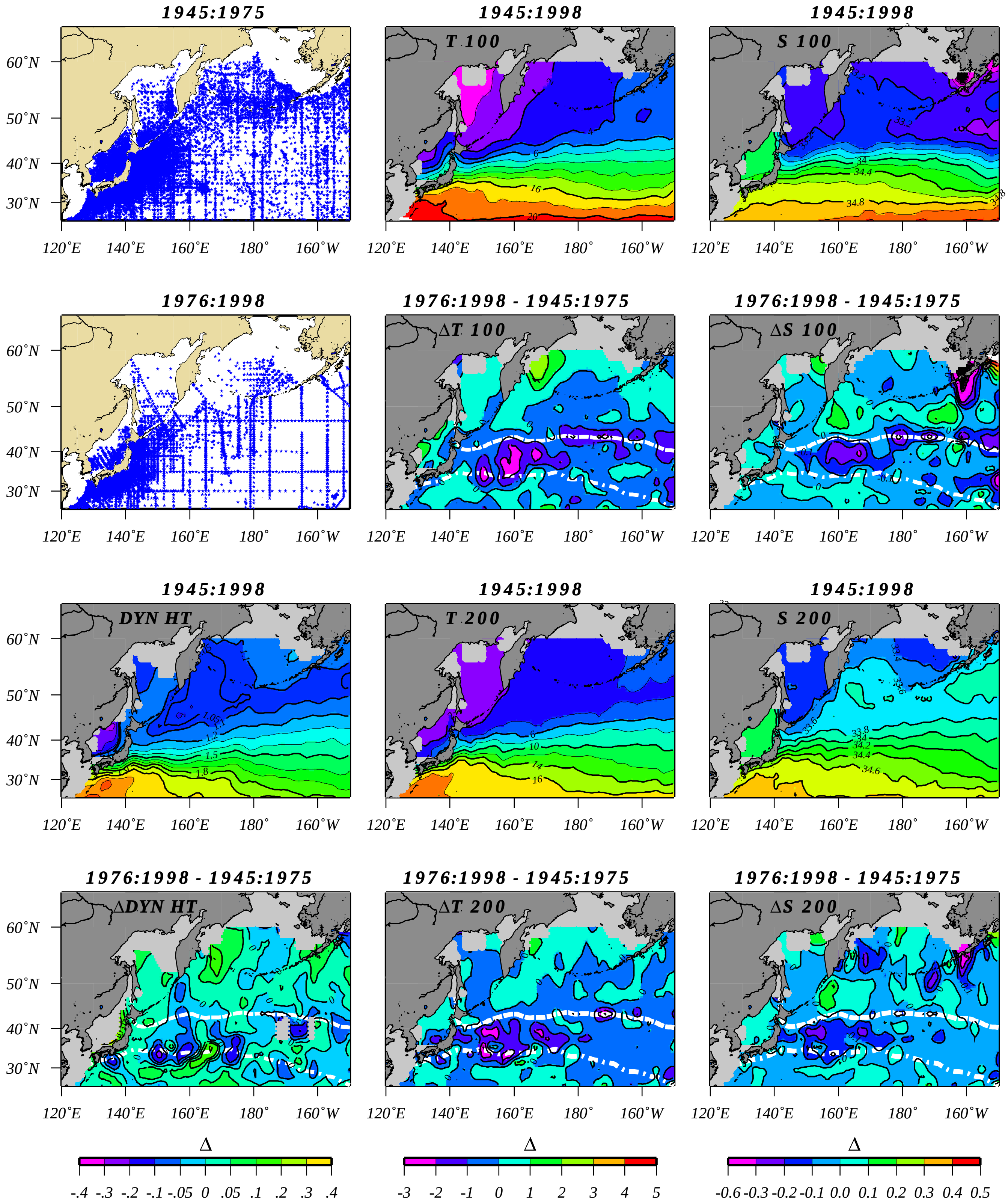
1945:1975
1945:1998
T 100
1945:1998
S 100
1976:1998
1976:1998 - 1945:1975
ΔT 100
1976:1998 - 1945:1975
ΔS 100
1945:1998
DYN HT
1945:1998
T 200
1945:1998
S 200
1976:1998 - 1945:1975
ΔDYN HT
1976:1998 - 1945:1975
ΔT 200
1976:1998 - 1945:1975
ΔS 200
60°N
50°N
40°N
30°N
120°E 140°E 160°E 180° 160°W
Δ
-.4 -.3 -.2 -.1 -.05 0 .05 .1 .2 .3 .4
Δ
-3 -2 -1 0 1 2 3 4 5
Δ
-0.6 -0.3 -0.2 -0.1 0.0 0.1 0.2 0.3 0.4 0.5

1945:1998

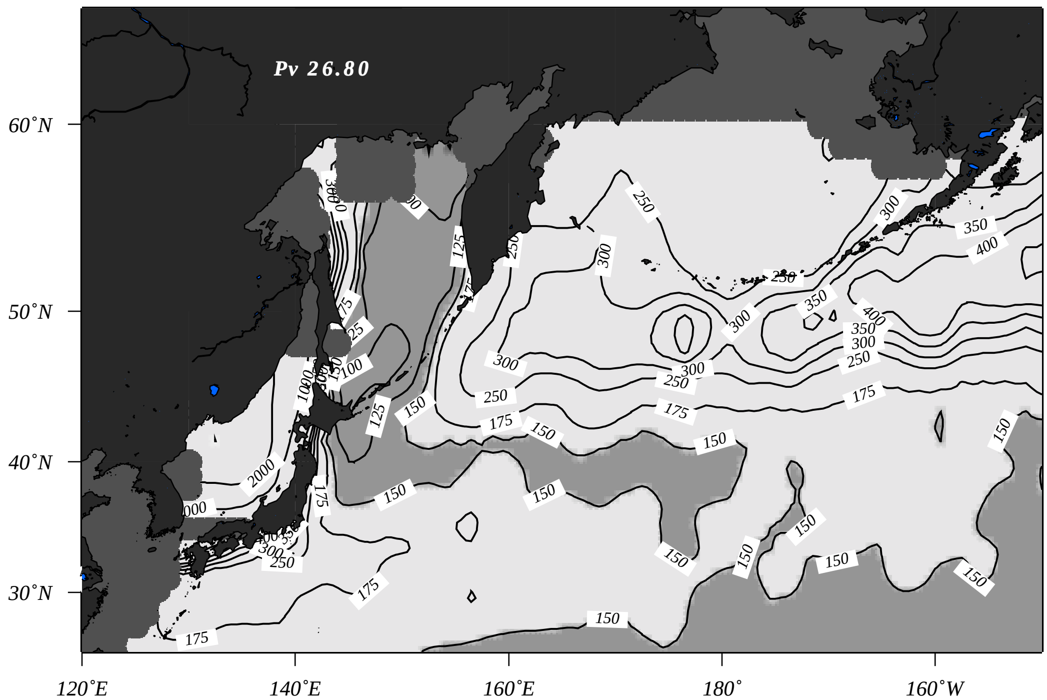

1976:1998 - 1945:1975

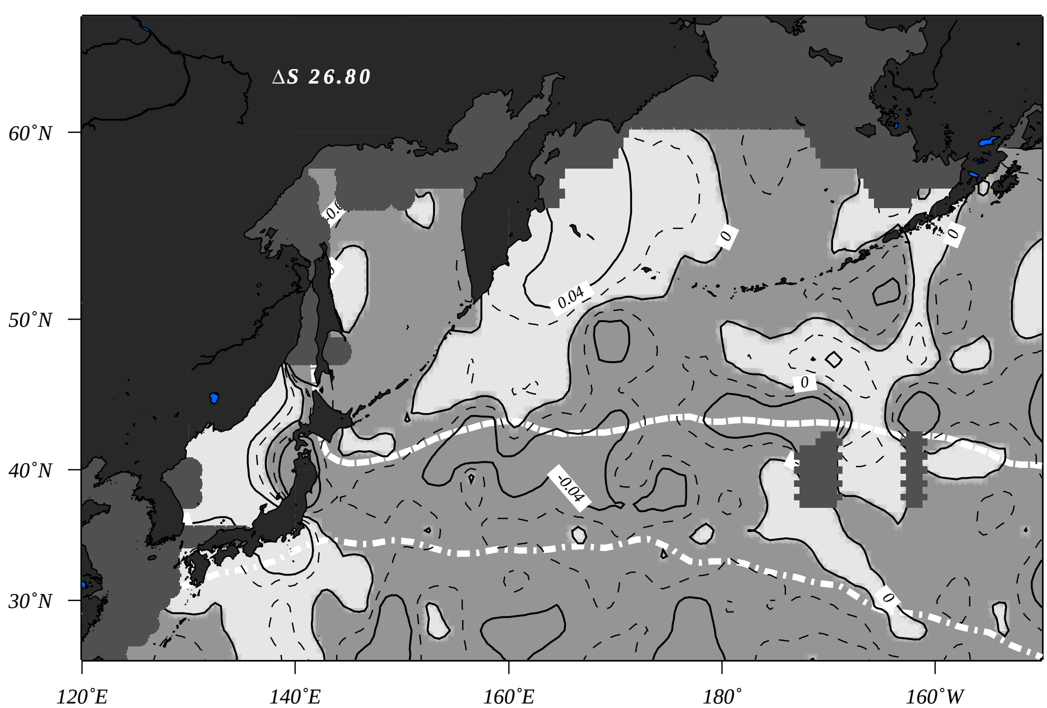

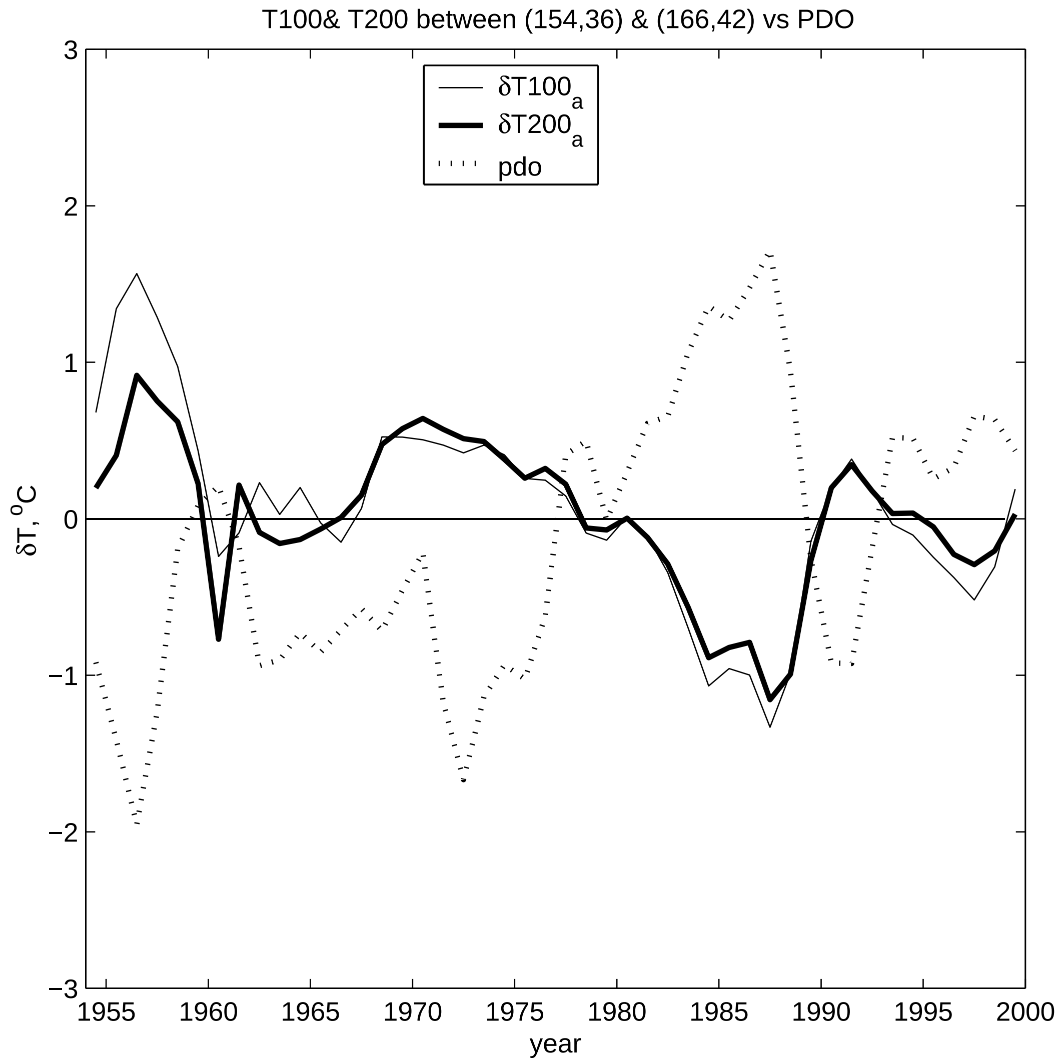
T100& T200 between (154,36) & (166,42) vs PDO
δT100a
δT200a
pdo
δT, °C
year
3
2
1
0
−1
−2
−3
1955
1960
1965
1970
1975
1980
1985
1990
1995
2000